THE JOURNAL OF PHYSICAL CHEMISTRY C

Article

pubs.acs.org/JPCC

Fluorine−Silicon Surface Reactions during Cryogenic and Near Room Temperature Etching

Stefan Tinck,* Erik C. Neyts, and Annemie Bogaerts

Research Group PLASMANT, Department of Chemistry, University of Antwerp, Universiteitsplein 1, B-2610 Antwerp, Belgium

ABSTRACT: Cyrogenic etching of silicon is envisaged to enable better control over plasma processing in the microelectronics industry, albeit little is known about the fundamental differences compared to the room temperature process. We here present molecular dynamics simulations carried out to obtain sticking probabilities, thermal desorption rates, surface diffusion speeds, and sputter yields of F, F_2, Si, SiF, SiF_2, SiF_3, SiF_4, and the corresponding ions on Si(100) and on SiF_{1-3} surfaces, both at cryogenic and near room temperature. The different surface behavior during conventional etching and cryoetching is discussed. F_2 is found to be relatively reactive compared to other species like SiF_{0-3}. Thermal desorption occurs at a significantly lower rate under cryogenic conditions, which results in an accumulation of physisorbed species. Moreover, ion incorporation is often observed for ions with energies of 30−400 eV, which results in a relatively low net sputter yield. The obtained results suggest that the actual etching of Si, under both cryogenic and near room temperature conditions, is based on the complete conversion of the Si surface to physisorbed SiF_4, followed by subsequent sputtering of these molecules, instead of direct sputtering of the SiF_{0-3} surface.

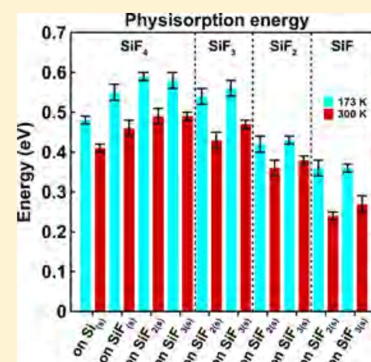

■ INTRODUCTION

Fluorine-based gases like SF_6, CF_4, and SiF_4 are commonly used in plasma processing for semiconductor manufacturing. Fluorine is very suitable for the etching of silicon, because it is the most reactive of all halogens on silicon. F atoms created in the plasma gradually convert the Si surface to volatile SiF_4 molecules. The actual removal of silicon from the surface is accelerated by ion bombardment.

The Si−F system has been relatively well studied experimentally, as reviewed by Winters and Coburn.[1] Also, a number of molecular dynamics (MD) results regarding the Si−F chemistry exist. It is noteworthy, however, that most investigations focus only on the mechanism(s) (e.g., influence of steric factors) of atomic fluorine interacting with silicon,[2−18] but they usually do not provide information on reaction rate (constants) or sputter yields, which is crucial information for the (plasma) modeling community.

Reports on sputter yields for the Si−F system are limited. Barone and Graves have calculated sputter yields with MD for Ar^+ ions bombarding a Si surface with varying degrees of fluorination.[19] Chiba et al. have reported sputter yields of F^+ ions with energies of 15, 30, and 100 eV on different SiF_x surfaces.[20]

Furthermore, chemical reaction probabilities are also scarcely reported. Reaction probabilities for F_2 on clean Si(100) are predicted by Carter and Carter,[21] while consecutive impacts of SiF_3, SiF_2, and SiF ions on Si(100) are investigated by Gou and co-workers.[22−25] Marcos et al. investigated the evolution of an etched Si surface under SF_6/O_2 plasma treatment with Monte Carlo simulations. They compared calculated etched trench profiles obtained with different predefined sticking coefficients for the F atoms and different SF_6/O_2 gas ratios to determine the role of the passivation layer and how it protects the sidewalls from undercutting effects.[26]

The purpose of the present study is to obtain a better understanding of the quantitative aspects of all reactions/processes that occur simultaneously during the etching of Si with various fluorine species. The goal of this work is therefore to answer questions like the following: (i) What is the probability that a certain species chemisorbs, physisorbs, or reflects as a function of chemical composition and temperature of the surface? (ii) What are the desorption and accumulation rates of physisorbed species as a function of surface temperature? (iii) How fast do species diffuse along the surface? (iv) What are the sputter yields of Si and F atoms as a function of ion type, ion energy, surface composition and surface temperature?

In addition, the innovation of this work is that we do not only calculate the various reaction probabilities for a conventional wafer temperature (i.e., near room temperature) but also for cryogenic conditions (i.e., −100 °C). Silicon cryoetching, proposed in 1988 by Tachi,[27] is currently most often used for etching silicon vias and 3D microelectronic components. The underlying mechanisms, however, are not yet fully understood, and in particular, the issue of how to control critical dimensions of microstructures is still unresolved.

The work presented in this report allows us to obtain a thorough understanding of which reactions occur during the etching process, not only at one specific condition but for a wide range of operating conditions. Also, we hope that the actual values for the sticking probabilities, desorption rates,

Received: October 30, 2014
Published: November 25, 2014

 © 2014 American Chemical Society dx.doi.org/10.1021/jp5108872 | J. Phys. Chem. C 2014, 118, 30315−30324

surface diffusion rates, and sputter yields of various species as a function of surface composition as presented in this work are of great value to the modeling community. Surface reaction probabilities are often not available or insufficiently known and they are indispensable when modeling plasmas with surface interactions. This is even more so for low-pressure plasmas (as commonly used in microchip development), where surface reactions can be more important than gas-phase collisions.

■ COMPUTATIONAL DETAILS

The calculations were performed with the classical molecular dynamics (MD) code LAMMPS.[29] In MD, forces on atoms are calculated on the basis of an interatomic potential to predict possible reaction mechanisms and trajectories of atoms. To describe the Si−F system, a combination of a Tersoff interatomic potential employing parameters developed by Abrams and Graves[30] and a long-range Lennard-Jones type van der Waals (vdW) interaction potential using parameters by Halgren[31] was used.

The Si−F Tersoff potential used in this work is constructed of a Tersoff-type binary potential energy function whose form is based on the Si−H potential of Murty and Atwater[32] but with parametrization for Si−F performed by Abrams and Graves.[30] The interested reader is referred to these references for a more detailed explanation of the applied equations and the specific parameters implemented for the Si−F system. In the Tersoff formalism, the total energy of the system is given by the sum of bond energies, where each bond between two atoms has attractive and repulsive components and where the bond energy is dependent on the angle with neighboring atoms. Inner and outer cutoff values for the Si−Si potential function are 2.7 and 3.0 Å, while the values for the Si−F and F−F functions are 1.84−2.14 and 1.7−2.0 Å, respectively.

The long-range vdW interactions are described by 12−6 Lennard-Jones type potential functions. More detailed information and the parameters specific for the Si−F system can be found in the mentioned paper by Halgren.[31] The inner cutoff values of the vdW potential functions are equal to the outer cutoff values of the Tersoff potentials used for Si−Si, Si−F, and F−F. A cosine-type spline function was applied to smoothly link both Tersoff and vdW potential functions together. The outer cutoff values for the F−F, Si−F, and Si−Si vdW interactions are 7, 9, and 11 Å, respectively.

So far, most MD results reported in the literature are obtained by using only a Tersoff potential for the Si−F system. This is sufficient when investigating the reaction mechanisms of bond breaking and formation during fluorination of Si. However, in reality, when a species arrives at a surface, its motion will be affected by long-range dispersion interactions near the surface. This may result in the species not immediately returning to the plasma (if no bonds are formed), which allows for the formation of a physisorbed layer. Desorption and accumulation rates of physisorbed species can therefore only be investigated with MD if these dispersion forces are considered in the interatomic potential. Indeed, whereas the cutoff range of the Tersoff potential is 4 Å, it is 11 Å in our current description (for Si−Si interactions). As will be discussed in the results section, these weak dispersion forces are the main reason for the significant differences observed in surface processes during etching at room temperature vs cryogenic temperature.

The difference in using only the Tersoff potential or a combination of both Tersoff and dispersion forces is illustrated in Figure 1.

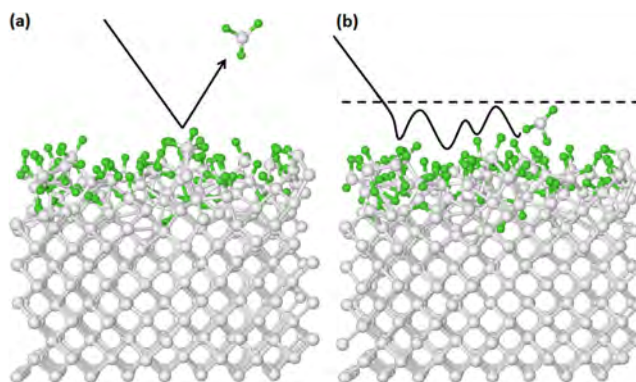

Figure 1. Illustration of the trajectory of a SiF_3 radical that is reflected from the surface when using the Tersoff potential (a) or a combination of the Tersoff potential and long-range dispersion forces (b). The area underneath the horizontal dashed line in part b illustrates the region where the radical is attracted toward the surface due to these dispersion forces. The white spheres are silicon atoms and the darker (green) spheres are fluorine atoms.

In Figure 1a, only the Tersoff potential is implemented and the plasma species (i.e., SiF_3 in this case) is immediately reflected from the highly fluorinated surface. In Figure 1b, long-range dispersion forces are included in addition to the Tersoff potential, and thus, the molecule is attracted toward the surface as long as it is within the range of the potential (i.e., below the dashed horizontal line). The SiF_3 species is also reflected, but it is pulled back toward the surface due to these dispersion forces. As a result, the physisorbed species diffuses over the surface until it chemisorbs or until it gains enough kinetic energy due to thermal fluctuations to move out of the attractive region near the surface and launch itself back into the plasma.

The potential implemented in LAMMPS was validated by comparing calculated bond lengths and energies with values from literature, as summarized in Table 1.

Table 1. Calculated Bond Energies and Lengths of the Si−F System in Comparison to Values from the Literature[33]

bond type	calcd bond energy (eV)	bond energy in lit. (eV)
Si−Si	2.66	2.31
F−F	1.60	1.60
Si−F	5.81	5.81
bond type	calcd bond length (pm)	bond length in lit. (pm)
Si−Si	232	233
F−F	141	142
Si−F	160	160

The simulation box consists of $21 \times 21 \times 15$ Å^3 Si(100) with periodic boundaries in the lateral directions. The positions of the atoms in the bottom monolayer of the silicon lattice were fixed to prevent displacement of the whole structure. The motion of all atoms was followed in the microcanonical ensemble using time steps of 1 fs for impacts of thermal species and 0.25 fs for impacts of ions (i.e., treated as fast neutrals).

In addition, five different surfaces of SiF, SiF_2, and SiF_3 (i.e., 15 in total) were created from the Si(100) structure by ion/neutral impacts of F and SiF_{1-4}. All these structures were thermalized at 300 or 173 K by employing a Berendsen heat bath with a coupling constant of 100 fs.[34]

Both nonconsecutive and consecutive impacts of Si, SiF, SiF_2, SiF_3, SiF_4, F, and F_2 species on all structures were investigated.

Table 2. Calculated Probabilities, as Well as the Corresponding Standard Deviations, for Immediate Sticking upon Impact of Various Impinging Species on Different Surfaces[a]

impinging species	on $Si_{(s)}$	on $SiF_{(s)}$	on $SiF_{2(s)}$	on $SiF_{3(s)}$
F	0.98/0.98 ± 0.01	0.92/0.93 ± 0.03	0.59/0.61 ± 0.05	0.23/0.25 ± 0.04
Si	1/1 ± 0	1/1 ± 0	0.41/0.40 ± 0.05	0.20/0.19 ± 0.04
SiF	0.88/0.89 ± 0.03	0.49/0.50 ± 0.05	0/0 ± 0	0/0 ± 0
SiF_2	0.51/0.50 ± 0.05	0.18/0.19 ± 0.04	0/0 ± 0	0/0 ± 0
SiF_3	0.37/0.37 ± 0.05	0.06/0.06 ± 0.02	0/0 ± 0	0/0 ± 0
SiF_4	0/0 ± 0	0/0 ± 0	0/0 ± 0	0/0 ± 0
F_2	1/1 ± 0	1/1 ± 0	0.77/0.77 ± 0.04	0.30/0.31 ± 0.05

[a]The surfaces are denoted with "(s)". For each combination, both of the values calculated at 300 and at 173 K are listed, separated by "/" (left = 300 K, right = 173 K).

Table 3. Calculated Probabilities, as Well as the Corresponding Standard Deviations, for Immediate Reflection upon Impact of Various Impinging Species on Different Surfaces[a]

impinging species	on $Si_{(s)}$	on $SiF_{(s)}$	on $SiF_{2(s)}$	on $SiF_{3(s)}$
F	0.02/0.02 ± 0.01	0.08/0.07 ± 0.03	0.41/0.39 ± 0.03	0.77/0.75 ± 0.04
Si	0/0 ± 0	0/0 ± 0	0/0 ± 0	0.04/0.04 ± 0.02
SiF	0.12/0.11 ± 0.03	0/0 ± 0	0/0 ± 0	0.26/0.25 ± 0.04
SiF_2	0/0 ± 0	0/0 ± 0	0/0 ± 0	0.16/0.16 ± 0.04
SiF_3	0/0 ± 0	0/0 ± 0	0/0 ± 0	0.11/0.12 ± 0.02
SiF_4	0/0 ± 0	0/0 ± 0	0/0 ± 0	0.06/0.06 ± 0.02
F_2	0/0 ± 0	0/0 ± 0	0/0 ± 0	0/0 ± 0

[a]The surfaces are denoted with "(s)". For each combination, both of the values calculated at 300 and at 173 K are listed, separated by "/" (left = 300 K, right = 173 K).

Regarding the nonconsecutive impacts, for each case, 100 impacts were simulated with a time of 12.5 ps per impact, which is appropriate to let the species sufficiently interact with the surface and to keep a reasonable computation time. For the consecutive impacts, 500 impacts per case were calculated with also 12.5 ps between two impacts. At the beginning of each impact, the incident species was introduced 15 Å above the center of the bulk surface, with a random direction of the initial velocity, allowing the species to interact with the surface at different locations and at different angles. For the neutrals, the thermal velocity was chosen from a Maxwellian distribution around 300 or 173 K with restrictions on the vertical velocity component to ensure that the species would always move toward the bulk. For the creation of the accumulated layer, as discussed in section 4, incident species were introduced 150 Å above the Si surface to allow the growth of a thick physisorbed layer. The ions were introduced in a similar matter, but vertical velocities (toward the bulk structure) were chosen from a Gaussian distribution around corresponding kinetic energies of 30, 100, 200, 300, 400, and 500 eV within a range of 10% of the defined energy, in order to mimic the ion fluxes in the case of applying a bias at the Si wafer.

■ RESULTS AND DISCUSSION

1. Surface Reaction Probabilities for Neutrals. In this section, probabilities for chemisorption (i.e., sticking) and reflection are reported. Physisorption is elaborated in section 3. The sticking probability of a certain species when arriving at a surface is defined as the probability that the species chemisorbs on the surface. In other words, the sticking probability is the probability that the species forms a chemical bond with a surface atom and hence does not reflect back into the plasma. Other possible reactions, apart from sticking, are reflection/desorption and physisorption. During reflection or desorption, the species is returned from the surface back into the gas phase. A physisorbed species is not attached to the surface by a chemical bond but is weakly bound to the surface by long-range dispersion forces like van der Waals interactions. These forces are typically weak, and physisorbed species can therefore diffuse over the surface until they find a site for chemisorption (e.g., a dangling bond of a surface atom) or find enough kinetic energy to desorb from the surface. So, two different types of chemisorption/sticking can be distinguished. The first is immediate sticking upon impact, where the species quickly creates a chemical bond with the surface upon arrival at the surface. The second is sticking of physisorbed species, which happens when the physisorbed species arrive at a site for chemisorption and which can occur much later than the initial moment of impact. While both types of sticking are dependent on the concentration of free sites for chemisorption and the eagerness of the species to chemically react with the surface, the second type (i.e., chemisorption of previously physisorbed species) is also dependent on the diffusion rate of the species along the surface. Indeed, if the species travels slowly over the surface, it will need a longer time to find a chemisorption site, and thus, it becomes more probable for this species to desorb after a certain time instead of chemisorb. On the other hand, a species that diffuses fast over the surface has a higher chance of finding a site for chemisorption before it finds enough energy to desorb. As this type of sticking can thus occur much later than the moment of impact, it is difficult to capture with MD due to the long time scales that must be covered. Of course, the definition of "immediate sticking" is ill-defined. For convenience, in this paper, we therefore consider the species to "immediately stick" if it creates a bond within 12.5 ps, which is the time covered for one impact in our simulations. In other words, if a species "immediately" sticks, it has created a bond with the surface near the impact location, and 12.5 ps is a proper time frame to have a good balance between allowing the species to sufficiently interact with the surface and having a

practical calculation time of a very large number of impacts for decent statistics. Trajectories of species covered over longer time scales will be discussed in more detail in section 3. In this section, we will discuss the probabilities for "immediate sticking", which provides information on the eagerness of the species to react with the different surfaces at 300 and 173 K.

Sticking probabilities of Si, SiF, SiF_2, SiF_3, SiF_4, F, and F_2 on surfaces with a chemical composition of SiF_{0-3} at 300 and 173 K were obtained by performing at least 100 nonconsecutive impacts per case and recording the different reactions that occurred. When necessary, more than 100 impacts were calculated to further improve the statistics. The calculated sticking probabilities are presented in Table 2.

A probability of 1 means that the species always immediately creates a bond with the surface upon impact (at least for all recorded impacts) and a probability of 0 means that a chemical bond was never formed within the time frame of 12.5 ps per impact. As discussed earlier, it should be realized that species that are not immediately chemisorbed can still be physisorbed, which might also result in sticking on a longer time scale. In these cases, the site for chemisorption can be far from the impact location. The sticking probabilities presented in Table 2 should thus be considered as the lower limits of sticking probabilities. Vice versa, the upper limits of the sticking probabilities can be obtained by observing the chances for reflection. Table 3 shows the probabilities for immediate reflection upon impact for all impinging species on the different surfaces.

Similar to the case for immediate sticking shown in Table 2, we would like to stress that the values presented in Table 3 are for immediate reflection and must be considered as the lower limits of the real reflection probability. Indeed, the total reflection probability is equal to the sum of the probability for immediate reflection, as shown here, and the probability for desorption after physisorption, which can occur much later in time compared to the moment of impact. This will be discussed in more detail in section 3.

From Tables 2 and 3 it can be concluded that the chemical behavior of the impinging species under cryogenic conditions is similar to the behavior at near room temperature, as all obtained probabilities for 300 and 173 K fall within the standard deviation. This is expected, since there is no barrier for chemisorption, and the temperature of the substrate and the kinetic energy of the impinging species thus have no influence on the immediate sticking behavior. In this case, the sticking coefficient is determined by steric factors.

As a general observation, it is clear that the immediate sticking probabilities gradually decrease when the surface is more fluorinated. This is expected because there are less dangling bonds available if the surface is more fluorinated, and hence, the surface becomes more repulsive for impinging species. This is in line with basic adsorption theory: if more sites are occupied with fluorine, fewer sites are available for chemisorption and thus the sticking probability will be lower.

Furthermore, in general, atoms are more reactive toward the surface than (stable) molecules. Although F atoms are indeed eager to create a chemical bond with the surface (see Table 2), it was observed that the sticking probabilities for F_2 are actually higher than those of the F atoms. This can be explained as follows. The F atoms are the lightest atoms in the system, so they have the highest impinging speed and due to their low mass, they can more easily escape the region above the surface where dispersion forces are active. Indeed, the chance for immediate reflection was found to be the highest for the (light) F atoms (see Table 3). The F atoms are actually the only species that can immediately reflect from the $Si_{(s)}$, $SiF_{(s)}$, and $SiF_{2(s)}$ surfaces. For the $SiF_{3(s)}$ surface, where very few adsorption sites exist, all species except F_2 can be reflected, but the escape probability decreases if the impinging species becomes heavier. The F atoms are often reflected into the plasma immediately after impact (probability of 0.77). The F_2 molecules, however, are not reflected immediately upon impact, but they spend more time diffusing along the surface due to their stronger dispersion interactions. Therefore, they reside longer on the surface, which increases the chance of finding a chemisorption site, hence explaining the higher sticking probability than for the F atoms (see Table 2). In addition, the F_2 bond is very weak (i.e., 1.6 eV; see Table 1) and it is thus more favorable to create Si−F bonds (i.e., bond energy of 5.81 eV), which also results in a high reactivity for F_2 molecules toward the silicon surface. During most impacts of F_2, it was observed that one F atom chemisorbs while the other F atom is reflected into the plasma.

Regarding the impinging SiF_x species, the sticking probability decreases with increasing fluorination degree of the impinging species (see Table 2), as expected. Indeed, in SiF the Si atom is only one-coordinated and thus has three free electrons to create a bond with the surface, while SiF_4 has no free sites. As a result, it is more probable for SiF to stick than for SiF_4. Since the Si−F bond is the strongest in this chemical system, SiF_4 will not easily break and create bonds with the surface, and hence, sticking was never observed for this molecule.

From Table 3 it is clear that the probabilities for immediate reflection on a highly fluorinated surface like $SiF_{3(s)}$ decrease with increasing molecular weight of the impinging species. Hence, even though SiF is a radical with three free electrons and will stick much more likely on the $Si_{(s)}$ and $SiF_{x(s)}$ surfaces than for instance SiF_4, it is still reflected more often on the $SiF_{3(s)}$ surface than SiF_4. As mentioned earlier, this is due to the fact that heavier species (consisting of more atoms) are subject to stronger dispersion interactions with the surface and therefore have a smaller chance of being reflected back into the plasma.

2. Sputter Yields. When a multicomponent surface is sputtered, it is likely that one element is sputtered faster than the other(s), a process often called preferential sputtering. A well-known example is that of SiO_2.[35] When a SiO_2 surface is sputtered, the oxygen atoms are removed preferentially, thus converting the surface to pure Si during sputtering. A similar effect is found here for sputtering SiF_x surfaces. It is observed that F atoms are removed with a higher yield compared to Si. Consequently, sputter yields for F and Si atoms are presented separately in Figures 2a−d and 3a−d, respectively.

Please note that in Figure 2a the negative values for the sputter yields correspond to yields for deposition (i.e., the values are always negative, indicating incorporation/deposition), because it is per definition impossible to sputter F atoms from a pure Si surface while, on the other hand, it is perfectly possible to incorporate F atoms in the Si layer by ion impacts.

Similar to the chemical behavior of the neutrals discussed in section 1, no significant difference was found in the sputter (or deposition) yields at 300 and 173 K. Since the ions arrive at the surface with energies of 30−500 eV, the energy difference of ~0.011 eV between both temperatures is too small to significantly affect the reaction yields.

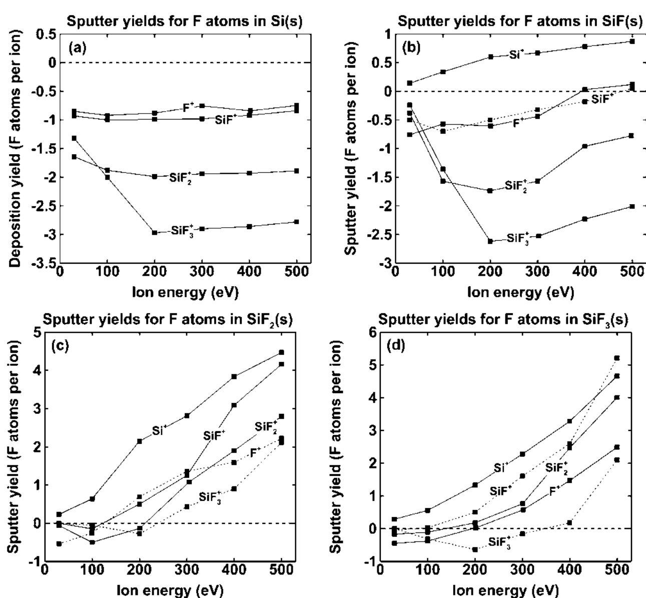

Figure 2. Calculated sputter yields of F atoms by various impinging ions on Si(100) (a), $SiF_{(s)}$ (b), $SiF_{2(s)}$ (c), and $SiF_{3(s)}$ (d). A negative sputter yield corresponds to atom deposition, where the ion impacts did not result in removal of atoms from the surface but in a net incorporation of atoms into the top surface layers. No significant difference was found between the sputter yields obtained at 300 and 173 K. SiF_4^+ and F_2^+ are not considered, as their density values in the plasma are close to zero and thus they have insignificant fluxes.

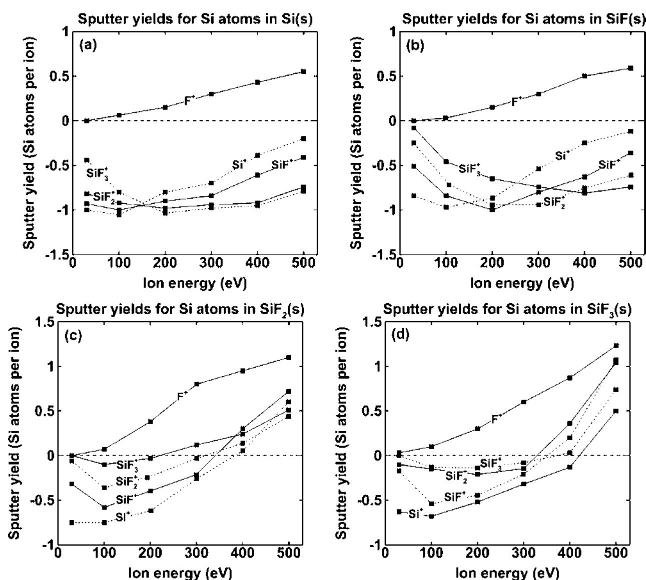

Figure 3. Calculated sputter yields of Si atoms by various impinging ions on Si(100) (a), $SiF_{(s)}$ (b), $SiF_{2(s)}$ (c), and $SiF_{3(s)}$ (d). A negative sputter yield corresponds to atom deposition, where the ion impacts did not result in removal of atoms from the surface but in a net incorporation of atoms into the top surface layers. SiF_4^+ and F_2^+ are not considered as their density values in the plasma are close to zero and thus they have insignificant fluxes.

As a general observation, it is clear that the sputter yield of both F and Si increases with fluorination degree of the surface. The sputter yield on $SiF_{3(s)}$ is higher than that on $SiF_{2(s)}$, and so on. For Si, this is because the more Si atoms that are fluorinated on the surface, the fewer bonds that they have with the underlying Si network, and therefore, they are more easily sputtered from the surface by ion impact. Similarly, the increasing sputter yield for F atoms with fluorination degree of the surface is because there are simply more F atoms present at the surface, which increases the chance for sputtering of fluorine.

It is interesting to note that most sputter yields do not simply increase with ion energy within the range of 30−500 eV but first decrease with rising energy (i.e., becomes more negative), followed by an increase at energies above ∼100−300 eV. This trend can be explained as follows.

At very low ion energies (i.e., <10 eV), the ion behaves much like its neutral equivalent. It has insufficient energy to sputter atoms or molecules from the surface and it also has insufficient energy to displace a lattice atom from the Si bulk and embed itself into the top surface layers. It was observed that these low-energy ions have a higher probability to immediately reflect from the surface instead of becoming physisorbed or chemisorbed. Indeed, because the ions arrive at the surface faster than the neutrals, they are also repelled more strongly upon impact and usually have enough kinetic energy left to launch back out of the region where the weak dispersion forces are significant, resulting in a smaller chance for remaining close to the surface and finally becoming chemisorbed. This explains why the net sputter yield or deposition yield is close to zero.

At higher ion energies (30−300 eV), it is observed that the ions practically always penetrate into the top few surface layers and remain there, occasionally sputtering other atoms or molecules from the surface in the process. As a result, most often no net removal of atoms from the surface is observed but rather net incorporation of atoms into the material. This is denoted in the figures by a negative sputter yield (i.e., a yield for depositing atoms). Note that the deposition yield can be larger than 1 (see Figure 2a,b), pointing out that more than one F atom is deposited per ion in the case of SiF_2^+ and SiF_3^+ bombardment.

When the ion energy increases even more (>400 eV), the ions also incorporate into the material, but the probability for removing other atoms from the surface increases due to a more aggressive collision cascade, which eventually leads to net sputtering of the surface.

Because all ions are accelerated toward the surface with more or less the same kinetic energy (corresponding to the applied bias voltage), the velocity of the heavier ions (like SiF_3^+) is lower than that of lighter ions, such as Si^+ or F^+. The speed at which the ions arrive at the surface is crucial for the subsequent sputter yield. Indeed, one fast atom can create a stronger collision cascade than a few "slow" atoms (like in the case for SiF_3^+). As a result, sputter yields of the larger ions are usually lower compared to those for the light ions. Note that this is true when the surface is effectively sputtered (i.e., at energies above 400 eV). As opposed to efficient sputtering, at lower ion energies, where mainly incorporation occurs (i.e., 300 eV and lower), these lighter ions have a higher chance for incorporation due to their higher speed, so the trends become reversed when moving from the deposition regime to the sputter regime.

Finally, it might surprise at first that the presented sputter yields in Figures 2 and 3 are low in general. For example, based on the presented yields, using 200 eV ions will always result in net ion incorporation instead of ion sputtering, while it is well-known that a silicon surface can be sputtered perfectly by 200 eV ions using a fluorine-based plasma. This is explained as follows.

In reality, the surface will actually first be converted to $SiF_{4(s)}$ before ion sputtering occurs, and SiF_4 is sputtered with a much higher yield, as it is only weakly bonded (i.e., physisorbed) on the surface. For typical wafer processing plasmas, the flux of neutrals is usually 100−1000 times higher than the ion flux.[36] As a result, the surface is always heavily fluorinated before sputtering occurs. It can be noted from Table 2 (section 1) that the probability to convert $SiF_{3(s)}$ to $SiF_{4(s)}$ is 0.11 and 0.3 for impinging F and F_2, respectively. Since their fluxes are a few orders of magnitude higher than the ion flux, it can be concluded that the surface is effectively converted to physisorbed SiF_4 molecules, which are very easily sputtered, even by low-energy ions. These observations are in line with basic ion-enhanced etching principles where a combination of chemical etching and ion sputtering yields a much higher etch rate than each process separately.[36]

Although direct sputtering of SiF_{0-3} surfaces might thus not occur often in reality, as the surface is usually converted to SiF_4 during etching, Figures 2 and 3 still give us important information on the behavior of the ions on the surface, like sputtering and incorporation yields. Indeed, because the layer of (physisorbed) SiF_4 molecules is easily removed by ion impact, the underlying SiF_{0-3} layers can still be reached by ions.

3. Desorption Rates and Surface Diffusion of Physisorbed Species. It must be noted from Table 3 that the probability for immediate reflection for the SiF_x species in most cases is 0 (or near 0 in the case of the $SiF_{3(s)}$ surface; see Table 3), while the sticking probabilities on the $SiF_{2(s)}$ and $SiF_{3(s)}$ surfaces are also (near) 0 (see Table 2). This suggests that the impinging SiF_x species most often become physisorbed without creating a chemical bond with the surface in the observed time for one impact, i.e., 12.5 ps (see above). A physisorbed species will thus travel over the surface for a certain period of time before it either reaches a site for chemical adsorption or is removed from the surface due to collisions resulting in sputtering or desorbs thermally after a certain period of time when it gains enough kinetic energy to be released from the surface and moves out of the region where the dispersion forces are significant. The time for a physisorbed species to do either can be much longer than the typical practical time scales covered in MD simulations, which presents some problems. Since it is computationally impractical to directly follow the trajectory of a physisorbed species until it sticks or desorbs, we attempt to predict in another way whether a physisorbed species will most likely desorb or find a site for chemisorption indirectly.

The chance for a physisorbed species to either desorb or stick after a certain period of time depends on its desorption rate and its rate of diffusion over the surface, respectively. The energy of physisorption can be obtained by recording the total potential energy of the system for two states, namely, an "adsorbed state", where the species is physisorbed on the surface, and a "separated state", where the species is far away from the surface having no dispersion interactions. The potential energy difference of both states yields the activation energy for desorption, provided we run both states for a long enough time to average out fluctuations in the recorded potential energy. The disadvantage of this method is that it is impossible to obtain the energy for physisorption if the species chemisorbs or reflects quickly upon impact, as the concept of physisorption is irrelevant for these situations. This was the case for F, Si, and F_2 on all surfaces and for all species on clean $Si_{(s)}$ and $SiF_{(s)}$, except for SiF_4. Indeed, as mentioned in section 1, it is observed that F, Si, and F_2 always quickly chemisorb or reflect after impact, while all species (except SiF_4) likely chemisorb on surfaces with high concentration of free sites, like $Si_{(s)}$ and $SiF_{(s)}$.

The physisorption energy is plotted for different species on different surfaces at 173 and 300 K in Figure 4.

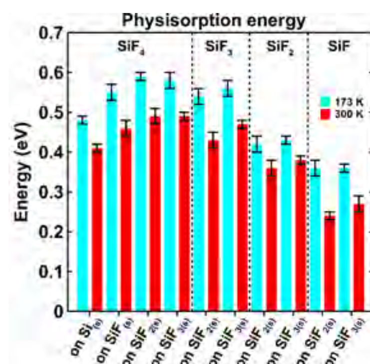

Figure 4. Calculated energy for desorption (i.e., physisorption energy) of physisorbed SiF_{1-4} on different surfaces, obtained at 173 and 300 K. Not all combinations could be obtained, as explained in detail in the text.

From Figure 4 it is clear that the energy needed for desorption decreases with decreasing size of the species. This is expected, since larger species contain more atoms that feel dispersion forces near the surface and are therefore more strongly adsorbed.

Furthermore, the chemical composition of the surface seems to have a minor effect on the desorption energy. Indeed, the calculated energies for desorption on $SiF_{2(s)}$ and $SiF_{3(s)}$ more or less coincide with each other within the standard deviation, for all species, whereas the values on $Si_{(s)}$ and $SiF_{(s)}$ (i.e., in the case of the SiF_4 molecules) are only slightly lower, again due to the lower dispersion forces, which is in turn due to less roughness of the layer. However, it is obvious that for all cases, the energy needed for the species to be desorbed from the surface is significantly higher under cryogenic conditions (i.e., 173 K) compared to at 300 K. Indeed, a higher temperature results in larger oscillation amplitudes between adsorbent and surface, leading to slightly larger average physisorption bond lengths and hence to overall weaker dispersion forces. This, in turn, leads to lower activation energies for desorption.

The actual rate constant of thermal desorption, which depends on the temperature of the surface and the activation energy (as calculated above), can now be estimated from the Arrhenius equation:

$$k = A\mathrm{e}^{-E_a/k_B T}$$

where k is the desorption rate constant (s^{-1}), A is the attempt frequency (s^{-1}), E_a is the activation energy or the energy barrier that needs to be overcome during desorption (eV), k_B is the Boltzmann constant, and T is the temperature (K). From this formula it is clear that species tend to remain on the surface for a longer time if the activation energy is higher and/or the surface temperature is lower. The latter is indeed true, since the activation energy is higher for lower temperatures, as shown in Figure 4.

The attempt frequency A can be obtained by monitoring the trajectory of the physisorbed species traveling over the surface and recording how many times they move upward (i.e., away

from the surface) before being pulled back, within a certain period of time. The attempt frequency, obtained in this way, typically has a value on the order of 10^{10}−10^{11} s^{-1}.

Thermal desorption is a slow process. This can be illustrated. For example, it can be deduced from Figure 4 that a SiF_4 molecule needs at least 0.4 eV to detach itself from a $Si_{(s)}$ surface at 300 K, which is about 20 times higher than the kinetic energy of the molecule at 300 K. Similarly, the same molecule needs about 0.49 eV to desorb from a $Si_{(s)}$ surface at 173 K, which is about 40 times higher than its kinetic energy at 173 K. It can thus be concluded that thermal desorption can occur only on the rare occasion when the kinetic energy of a surface atom interacting with the physisorbed SiF_4 is large enough (i.e., high-energy end of the Maxwell distribution) to launch the SiF_4 molecule in the gas phase, away from the surface.

Naturally, this process will occur less often under cryogenic conditions. As an example, we illustrate the difference in desorption rate constant of physisorbed SiF_2 on $SiF_{3(s)}$. We selected this example because the activation energy difference between 173 and 300 K was found to be the smallest here, of all situations investigated (see Figure 4 above); hence, all other cases will yield an even larger difference between cryogenic and room temperature. For an attempt frequency of 5×10^{10} s^{-1}, the desorption rate constant at 173 K is 0.015 s^{-1}, while it is about 20 600 s^{-1} at 300 K. As desorption is a zero-order reaction, the desorption rate is equal to the desorption rate constant. Hence, the desorption rate for species at room temperature is at least 1 million times higher than under cryogenic conditions. This suggests that accumulation of physisorbed species is more likely to occur at lower surface temperatures, as will be discussed in more detail in section 4.

As mentioned above, the chance for a physisorbed species to either desorb or stick after a certain period of time depends not only on its desorption rate but also on its rate of diffusion over the surface. The rate of surface diffusion of physisorbed species was obtained by monitoring the trajectory of the species as they travel over the surface and recording the mean-squared displacement (MSD). The MSD is a measure for how far the species travel from the location where they first come into contact with the surface. The slope of the MSD versus time is proportional to the diffusion coefficient, which is an indirect measure of the surface diffusion rate. Figure 5 illustrates the surface diffusion coefficients of SiF_4 on various $SiF_{x(s)}$ surfaces recorded at 300 and 173 K. The diffusion coefficients of the other species are also summarized in Table 4.

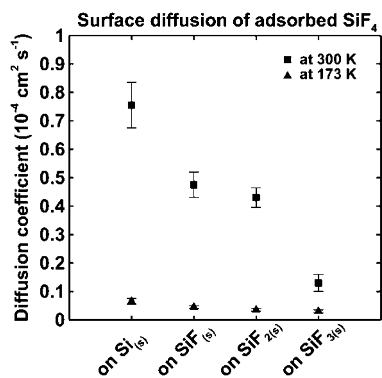

Figure 5. Calculated diffusion coefficients for physisorbed SiF_4 on different SiF_x surfaces, obtained at 173 and 300 K.

From Figure 5 and Table 4 it is clear that the surface diffusion coefficient is considerably lower (i.e., often 1 order of magnitude) at 173 K compared to 300 K, which is logical. It was observed that even in the case of physisorption, the traveling speed is far from constant but rather "stepwise", meaning that the molecule usually resides in a certain location before quickly moving to another location and residing there again for a relatively long time, and so on. Due to the less pronounced oscillations of atoms at cryogenic temperature, it is less likely for the physisorbed species to be pushed further along the surface, explaining why the diffusion rate is significantly lower at cryogenic temperature.

Also, the surface diffusion coefficients decrease with increasing size of the physisorbed species. Indeed, SiF_4 travels more slowly than SiF_3, and so on. Due to the stronger dispersion forces present for larger molecules, it is more difficult for these species to "jump" to different locations on the surface, resulting in a lower overall travel distance within a given time.

Furthermore, it seems that the diffusion coefficient is also dependent on the chemical composition of the surface, or rather the surface roughness. The more fluorinated the surface, the more amorphous and rough it becomes, creating more energetically interesting spots for the physisorbed molecules to reside before jumping to another location, resulting in lower diffusion coefficients.

Finally, when we compare our calculated surface diffusion coefficients (as a measure for the speed of surface diffusion) with the desorption rates, at 300 and 173 K, we can conclude that the difference in diffusion speeds (i.e., at maximum 1 order of magnitude) is much smaller than the difference in desorption rates (i.e., at minimum 6 orders of magnitude, as shown for the example above). It is thus clear that the probability for a physisorbed species to finally find a site for chemisorption, after diffusing over the surface, is much higher under cryogenic conditions than at room temperature, although most species simply remain physisorbed for quite a long time. This will be elaborated in more detail in section 4 below.

4. The Difference between Conventional Etching and Cryoetching. In previous sections it was demonstrated that the chemical behavior of the neutral species (section 1) and the sputter yields of the ions (section 2) are virtually identical for room temperature and cryogenic conditions. However, there is a large difference in the behavior of the physisorbed species between both temperatures. Indeed, from section 3 it can be concluded that the diffusion rate is mostly about 1 order of magnitude higher at room temperature compared to cryogenic conditions, but this difference is much smaller than the difference in desorption rate, which can span 6 orders of magnitude (or more), as shown for the example of physisorbed SiF_2 on $SiF_{3(s)}$ (see section 3 above). This suggests that, under cryogenic conditions, a physisorbed species will practically always find a site for chemisorption when diffusing along the surface before it finds enough energy to desorb. On the other hand, at room temperature the species will most likely desorb before reaching a site for chemisorption. This eventually results in an overall higher sticking probability for neutral species under cryogenic conditions.

Furthermore, for wafer processing, usually low-pressure plasmas are applied, where less than 1% consists of charged species or reaction products. Thus, often more than 99% of the species that arrive at the surface are background gas molecules like CF_4, SF_6, or SiF_4, which usually have no or low reactivity

Table 4. Calculated Surface Diffusion Coefficients (10^{-4} cm^{-2} s^{-1}) of the Adsorbed Species on Different $SiF_{x(s)}$ Surfaces, for 300 and 173 K

adsorbed species	on $Si_{(s)}$	on $SiF_{(s)}$	on $SiF_{2(s)}$	on $SiF_{3(s)}$
		300 K		
F	[a]	[a]	[a]	[a]
Si	[a]	[a]	[a]	[a]
SiF	[a]	[a]	1.20 ± 0.11	0.63 ± 0.07
SiF_2	[a]	[a]	0.61 ± 0.09	0.38 ± 0.06
SiF_3	[a]	[a]	0.46 ± 0.04	0.25 ± 0.04
SiF_4	0.76 ± 0.08	0.46 ± 0.05	0.43 ± 0.03	0.13 ± 0.03
F_2	[a]	[a]	[a]	[a]
		173 K		
F	[a]	[a]	[a]	[a]
Si	[a]	[a]	[a]	[a]
SiF	[a]	[a]	0.15 ± 0.02	0.09 ± 0.02
SiF_2	[a]	[a]	0.10 ± 0.02	0.08 ± 0.01
SiF_3	[a]	[a]	0.08 ± 0.01	0.07 ± 0.01
SiF_4	0.07 ± 0.01	0.045 ± 0.005	0.035 ± 0.005	0.030 ± 0.005
F_2	[a]	[a]	[a]	[a]

[a]The surface diffusion coefficients could not be obtained for these situations because the adsorbed species quickly chemisorb/react with the surface (cf. sticking coefficients in Table 2), preventing the derivation of a proper diffusion coefficient.

toward the silicon surface and will therefore most likely physisorb. Under typical wafer processing conditions (e.g., a pressure of 50 mTorr), the flux of the neutral species toward the surface is on the order of 10^{18} cm^{-2} s^{-1}, which yields a time between impacts of ~0.02 ms on the surface area defined in our MD simulations (i.e., 441 Å^2). If we compare this time between impacts with the residence times of SiF_4 on $Si_{(s)}$ at 173 and 300 K (i.e., 960 s and 0.07 ms, respectively, estimated from the desorption rates; cf. section 3 above), it can be concluded that at 173 K SiF_4 molecules can easily accumulate because the residence time is much longer than the time between impacts. On the other hand, at 300 K, the residence time is on the order of sub-milliseconds, so the SiF_4 molecules will most likely thermally desorb before another SiF_4 molecule from the plasma arrives at that surface site. Please note that the time for desorption in this example is still slightly longer than the time between impacts (i.e., 0.07 ms compared to 0.02 ms), but once a monolayer of physisorbed SiF_4 molecules is formed, other arriving SiF_4 molecules will always desorb long before the next impact because dispersion forces become weaker if the accumulated layer is less dense.

Finally, Figure 6 illustrates an accumulated layer of physisorbed SiF_4 molecules on Si(100) under cryogenic conditions.

As mentioned earlier, the plasma consists of more than 99% of background gas, so we can assume that the physisorbed layer consists practically solely of non- or low-reactive molecules like SiF_4. Since there are no chemical bonds between the SiF_4 molecules, the accumulated layer is only kept together by weak dispersion interactions, which make the layer very dynamic and easily removable by ion impact. Indeed, our calculations predict that 30 eV ions practically completely disintegrate the accumulated layer by causing a collision cascade that gives most of the physisorbed SiF_4 molecules enough kinetic energy to launch themselves back into the plasma.

Because the flux of neutrals is typically 1000 or more times larger than the ion flux under typical wafer processing conditions,[36] it is expected that an accumulated layer will again be formed before the next ion arrives on that surface site. Even though the sputter yields at cryogenic and room temperature conditions are the same (see section 2), sputtering of the underlying Si layer might be slightly inhibited during cryoetching by the formation of this accumulated layer of physisorbed neutrals that assimilate a part of the ion energy and thus lower the chance for sputtering of the underlying silicon.

It can therefore be concluded that the relatively weak dispersion interactions are responsible for creating a strong difference in the surface behavior of the fluorine−silicon system. However, due to the small difference in sputter yield (with or without the accumulated layer), the actual difference in etch rate is expected to be not very pronounced, which is indeed also experimentally observed.[28]

■ CONCLUSIONS

Molecular dynamics simulations have been performed to obtain a better insight in the reaction probabilities, sputter yields, thermal desorption rates, and surface diffusion rates of relevant species in the Si−F chemical system on Si surfaces with varying degrees of fluorination, both for conventional near room temperature etching and cryoetching.

It was found that sticking probabilities decrease with an increasing degree of fluorination of the surface and that F_2 is very reactive toward the Si surface. The chemical behavior of the species was found to be identical for both room temperature and cryogenic conditions. However, large differences are found in the behavior of the physisorbed species.

The sputter yields are found to increase with the degree of fluorination of the surface, as expected. However, the sputter yields are often negative and decrease with ion energy in the range of 30−200 eV. This can be explained by a higher probability for ion incorporation instead of sputtering of the surface. Furthermore, light atoms like Si^+ and F^+ are more efficient at sputtering the $SiF_{0-3(s)}$ surface due to their higher speed compared to the SiF_{1-3}^+ ions.

Comparing the obtained sputter yields with the calculated sticking probabilities, it can be concluded that the actual etching of silicon with fluorine occurs by first converting the Si surface to physisorbed SiF_4 followed by subsequent sputtering, rather than direct sputtering of the $SiF_{0-3(s)}$ layer.

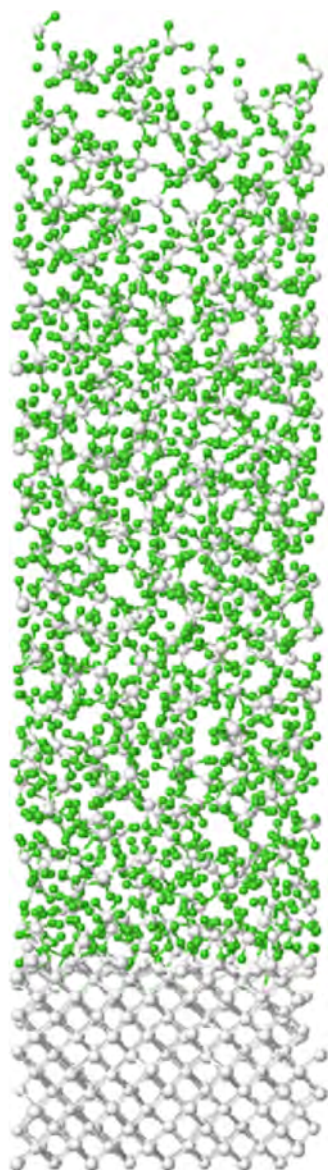

Figure 6. Illustration of an accumulated layer of physisorbed SiF_4 molecules on a Si(100) surface at 173 K. There are no chemical bonds between the SiF_4 molecules (i.e., no network). The layer is kept together only by weak dispersion forces and its height fluctuates strongly.

The desorption rate of physisorbed species decreases with increasing species size but was found to be more or less unaffected by the surface composition and roughness. Under cryogenic conditions, the desorption rate can be many orders of magnitude lower compared to that at room temperature, suggesting a high probability for the formation of an accumulated layer of physisorbed species.

Surface diffusion was found to decrease with increasing species size and surface roughness, and the diffusion coefficient is typically about 1 order of magnitude lower for cryogenic temperatures compared to room temperature.

Finally, due to the formation of an accumulated layer of physisorbed SiF_4 at 173 K but not at 300 K, it can be concluded that the weak dispersion forces are responsible for creating a difference in surface behavior between cryogenic and room temperature etching. However, in spite of this accumulated layer under cryogenic conditions, the sputter yield is almost not influenced by this layer, resulting in quite similar etch rates, as is found experimentally.

AUTHOR INFORMATION

Corresponding Author

*E-mail: stefan.tinck@uantwerpen.be.

Notes

The authors declare no competing financial interest.

ACKNOWLEDGMENTS

The Fund for Scientific Research Flanders (FWO) is acknowledged for financial support of this work. This work was carried out in part using the Turing HPC infrastructure at the CalcUA core facility of the Universiteit Antwerpen, a division of the Flemish Supercomputer Center VSC, funded by the Hercules Foundation, the Flemish Government (department EWI), and the University of Antwerp.

REFERENCES

(1) Winters, H. F.; Coburn, J. W. Surface Science Aspects of Etching Reactions. *Surf. Sci. Rep.* **1992**, *14*, 161.
(2) Yarmoff, J. A.; McFeely, F. R. Mechanism of Ion Assisted Etching of Silicon by Fluorine Atoms. *Surf. Sci.* **1987**, *184*, 389.
(3) Humbird, D.; Graves, D. B. Atomistic Simulations of Spontaneous Etching of Silicon by Fluorine and Chlorine. *J. Appl. Phys.* **2004**, *96*, 791.
(4) Humbird, D.; Graves, D. B. Molecular Dynamics Simulations of Si−F Surface Chemistry with Improved Interatomic Potentials. *Plasma Sources Sci. Technol.* **2004**, *13*, 548.
(5) Darcy, A.; Galijatovic, A.; Barth, R.; Kenny, T.; Krantzmann, K. D.; Schoolcraft, T. A. Molecular Dynamics Simulations of Silicon−Fluorine Etching. *J. Mol. Graphics* **1996**, *14*, 260.
(6) Gadiyak, G. V.; Morokov, Y. N.; Mukhin, D. N. Simulation of Fluorine Interaction with a Silicon Surface. *Appl. Surf. Sci.* **1992**, *60*, 131.
(7) Youngman, R. E.; Sen, S. Structural Role of Fluorine in Amorphous Silica. *J. Non-Cryst. Solids* **2004**, *349*, 10.
(8) Lo, C. W.; Varekamp, P. R.; Shuh, D. K.; Durbin, T. D.; Chakarian, V.; Yarmoff, J. A. Substrate Disorder Induced by a Surface Chemical Reaction: The Fluorine−Silicon Interaction. *Surf. Sci.* **1993**, *292*, 171.
(9) Yang, C.; Kang, H. C.; Tok, E. S. Adsorption and Coadsorption of Hydrogen and Fluorine on the Si(100)-(2 × 1) Surface. *Surf. Sci.* **2000**, *465*, 9.
(10) Humbird, D.; Graves, D. B. Improved Interatomic Potentials for Silicon−fluorine and Silicon−Chlorine. *J. Chem. Phys.* **2004**, *120*, 2405.
(11) Ezaki, T.; Ohno, T. Theoretical Investigations of Adsorption of Fluorine Atoms on the Si(100) Surface. *Surf. Sci.* **2000**, *444*, 79.
(12) Silverman, A.; Adler, J.; Weil, R. Computer Modelling of the Diffusion Mechanisms of Fluorine in Amorphous Silicon. *Thin Solid Films* **1990**, *193*, 571.
(13) Brault, P. Fluorine Diffusion In Silicon Under Plasma Treatment. *J. Phys.: Condens. Matter* **1991**, *3*, 7073.
(14) Radny, M. W.; Smith, P. V. Half Monolayer and Monolayer Chemisorption of Fluorine on the Silicon(001) 2 × 1 Surface. *Surf. Sci.* **1994**, *301*, 97.
(15) Radny, M. W.; Smith, P. V. Chemisorption of Fluorine on the Silicon(001) 2 × 1 Surface. *Vaccuum* **1994**, *45*, 293.
(16) Carter, L. E.; Carter, E. A. Simulated Reaction Dynamics of F Atoms on Partially Fluorinated Si(100) Surfaces. *Surf. Sci.* **1996**, *360*, 200.
(17) Weakliem, P. C.; Carter, E. A. Surface Chemical Reactions Studied via Ab Initio-Derived Molecular Dynamics Simulations: Fluorine Etching of Si(100). *J. Chem. Phys.* **1993**, *98*, 737.
(18) Walch, S. P. Computed Energetics For Etching of the Si(100) Surface by F and Cl Atoms. *Surf. Sci.* **2002**, *496*, 271.

(19) Barone, M. E.; Graves, D. B. Chemical and Physical Sputtering of Fluorinated Silicon. *J. Appl. Phys.* **1995**, *77*, 1263.
(20) Chiba, S.; Aoki, T. Matsuo, Molecular Dynamics Simulation of Fluorine Ion Etching of Silicon. J. *Nucl. Inst. Methods Phys. Res., Sect. B* **2001**, *180*, 317.
(21) Carter, L. E.; Carter, E. A. F_2 Reaction Dynamics with Defective Si(100): Defect-Insensitive Surface Chemistry. *Surf. Sci.* **1995**, *323*, 39.
(22) Gou, F.; Xie, Q.; Zhu, L.; Weili, S.; Ming, X. Interaction Of SiF_3 With Silicon Surface: Molecular Dynamics Simulation. *Nucl. Inst. Methods Phys. Res., Sect. B* **2006**, *248*, 113.
(23) Gou, F.; Ming, X.; Weili, S.; Chen, T. Deposition of Amorphous Fluorosilane Thin Film on Silicon Surface: Atomic Simulation. *J. Non-Cryst. Solids* **2007**, *353*, 4186.
(24) Chen, X.; Lu, X.; He, P.; Zhao, C.; Sun, W.; Zhang, P.; Gou, F. Deposition and Etching of SiF_2 on Si Surface: MD Study. *Phys. Proc.* **2012**, *32*, 885.
(25) Gou, F. Molecular Dynamics Simulation of Deposition and Etching of Si Bombarding by Energetic SiF. *Appl. Surf. Sci.* **2007**, *253*, 5467.
(26) Marcos, G.; Rhallabi, A.; Ranson, P. Monte Carlo Simulation Method for Etching of Deep Trenches in Si by a SF_6/O_2 Plasma Mixture. *J. Vac. Sci. Technol. A* **2003**, *21* (1), 87.
(27) Tachi, S.; Tsujimoto, K.; Okudaira, S. Low-Temperature Reactive Ion Etching and Microwave Plasma Etching of Silicon. *Appl. Phys. Lett.* **1988**, *52*, 616.
(28) Dussart, R.; Tillocher, T.; Lefaucheux, P.; Boufnichel, M. Plasma Cryogenic Etching of Silicon: From the Early Days to Today's Advanced Technologies. *J. Phys. D: Appl. Phys.* **2014**, *47*, 123001.
(29) Plimpton, S. Fast Parallel Algorithms for Short-Range Molecular Dynamics. *J. Comput. Phys.* **1995**, *117*, 1 (http://lammps.sandia.gov).
(30) Abrams, C. F.; Graves, D. B. Molecular Dynamics Simulations of Si Etching by Energetic CF_3^+. *J. Appl. Phys.* **1999**, *86*, 5938.
(31) Halgren, T. A. The Representation of van der Waals (vdW) Interactions in Molecular Mechanics Force Fields: Potential Form, Combination Rules, and vdW Parameters. *J. Am. Chem. Soc.* **1992**, *114*, 7827.
(32) Murty, M. V. H.; Atwater, H. A. Empirical Interatomic Potential for Si−H Interactions. *Phys. Rev. B* **1995**, *51*, 4889.
(33) Benson, S. W. Bond Energies. *J. Chem. Educ.* **1965**, *42*, 502.
(34) Berendsen, H. J. C; Postma, J.; Van Gunsteren, W.; Dinola, A.; Haak, J. Molecular Dynamics with Coupling to an External Bath. *J. Chem. Phys.* **1984**, *81*, 3684.
(35) Kim, D. H.; Lee, G. H.; Lee, S. Y.; Kim, D. H. Atomic Scale Simulation of Physical Sputtering of Silicon Oxide and Silicon Nitride Thin Films. *J. Cryst. Growth* **2006**, *286*, 71.
(36) Tinck, S.; Boullart, W.; Bogaerts, A. Simulation of an Ar/Cl_2 Inductively Coupled Plasma: Study of the Effect of Bias, Power and Pressure and Comparison With Experiments. *J. Phys. D: Appl. Phys.* **2008**, *41*, 065207.